Chalcogenide Letters Vol. 21, No. 5, May 2024, p. 413 - 421

Mechanical, magnetic, and electronic characteristics of Sm-based chalcogenides for spintronics and device applications

N. A. Noor[a,*], F. Nasrullah[a], Ihab M. Moussa[b], S. Mumtaz[c]
[a]*Department of Physics, RIPHAH International University, Campus Lahore, Pakistan*
[b]*Department of Botany and Microbiology, College of Science, King Saud University, P.O. Box 2455, Riyadh, 11451, Saudi Arabia*
[c]*Electrical and Biological Physics, Kwangwoon University, Seoul, 01897, South Korea*

To comprehend the mechanical, electronic, and magnetic properties of chalcogenides $HgSm_2S/Se_4$, a DFT-oriented thorough investigation is carried out. The elastic constants and spin-dependent electrical characteristics are determined by using the PBEsol-GGA functional and (mBJ) potential correspondingly. Through optimization, a sufficient amount of energy is discharged by the FM state as compared to nonmagnetic states. By investigating Born stability criteria and formation energy, the structural stabilities of both spinels are verified. The calculated Poisson's and Pugh's ratios showed that both spinels are ductile. The estimation of Curie temperature has supported the existence of a ferromagnetic nature at room temperature. Moreover, the presence of ferromagnetism in both spinels is confirmed by spin-oriented electrical characteristics, owing to the coupling between component states associated with Sm and S/Se.

(Received February 13, 2024; Accepted May 13, 2024)

Keywords: Chalcogenide spinels, First-principle calculations: Curie temperature, Mechanical properties, Half-metallic ferromagnetism

1. Introduction

Owing to properties like reliability, strong core electronic conductivity, and unanticipated phase intensity, Strong thiospinel frameworks in the cubic Fd-3m space group are particularly noteworthy [1-3]. In octahedral patterns (O^{2-}, S^{2-}, and Se^{2-}), the bonding amongst the B-cations, as well as Y-anions chalcogenide, conduces to spinel compounds having composition AB_2X_4. In a three-dimensional framework created by edge-sharing ABX_6 octahedral, tetrahedrally coordinated positions are inhabited by A-cations. Good chemical and thermal stability as well as significant electromagnetic properties are remarkably inherent in the majority of spinels [4], one of the applications of chalcogenides that resemble mixed metal spinel is to function as catalysts in a variety of procedures. Moreover, these are useful in redox processes to address power concerns on account of their superior chemical and physical properties [5]. Ferromagnetic spinels also play a vital role in the production of spintronic applications, proving them particularly interesting substances [6-8]. Such materials acquired technical and scientific uses in microelectronic devices through the modification of their intrinsic spin orientation feature, which allows for a variety of data processing and storage operations [9, 10].

Semiconducting and ferromagnetic compounds are thought to be very advantageous technologies. Spintronic properties can be improved by doping certain semiconducting substances [11-12]. The most ancient known magnetic semiconductors are thought to be the compounds having composition AB_2Z_4 (Z = S, Se, A= Mg, Zn, B = Sm based atoms) [13, 14]. A comparative study of these spinels to compounds like $MgYb_2S_4$ depicted better ferromagnetic behavior in spinels [15]. However, spinels with significant ferromagnetic traits are widely used in memory and

* Corresponding authors: naveedcssp@gmail.com
https://doi.org/10.15251/CL.2024.215.413

spintronic applications [16, 17]. Material researchers are especially fascinated with rare-earth-based spinels in view of their ferromagnetic characteristics leading to enormous magneto-resistance [18, 19]. Magnetic field sensors, biosensors, RAM, and multiple electronic appliances are novel applications on account of their gigantic magneto-resistive distinctive features. The working of electronic devices can be powered by the spinels' synchronous execution of electric charge and spin.

The comprehensive study on Magnesium cells reported them as an excellent framework for researching the Mg^{2+} intercalation process, but their insufficient operating voltages proved them incapable of achieving significant energy density. The solid-state electrolytes that comprise spinels containing Mg^{2+}, such as $MgTm_2S_4$ and $MgTm_2Se_4$, are employed under their great structural durability with E_{hull} value of less than 50 meV/atom [20, 21]. Through a thorough investigation, we came to know that there has been no experimental research history on $HgSm_2S/Se_4$ spinels. In this letter, we have conducted an in-depth theoretical investigation of $HgSm_2S/Se_4$ to study the mechanical, optoelectronic, and magnetic characteristics by using the DFT-oriented WIEN2k program [22]. This is because it can be harder to disclose accurate electronic characteristics of the spinels indicating novel applications [23, 24].

2. Research methodology

The spin-polarized physical properties of $HgSm_2S/Se_4$ are examined by means of the FP-LAPW+lo method coupled with the WIEN2k software package. PBEsol-GGA is used to calculate mechanical and structural properties amid numerous calculations for determining V_{XC}[25]. Under the umbrella of the density functional theory approach, the PBEsol-GGA approximation operates as an outstanding exchange-correlation functional. In order to calculate the semiconductor band gaps appropriately, the electronic characteristics are estimated via mBJ potential [26-28]. To get precise details of structures that modulate the crystal structural behavior of the concerned composition, a reduction will occur in internal forces (reduced <1mRy/au). The valence electron calculations appeared quasi-reliant in comparison to the core electrons, which resided at a relativistic stage, as demonstrated using the FP-LAPW approach. For both spinels, the cut-off energy value required to distinguish the valence from the core states at the specific level was 6.0Ry. When it comes to the energy convergence requirement, the reciprocal lattice's $R_{MT}\times Kmax = 8$ chemical formula represents the increment in the uttermost values of Kmax, the wave vector, and R_{MT}, the muffin-tin radius. Additionally, the peak point of the Gaussian factor, Gmax = 22, and that of lmax = 10, were measured. In order to improve (SCF), we constructed 2000 k-points utilizing a 12×12×12 k mesh grid in Ist BZ.

3. Discussion on results

In this letter, first, we discussed the structural stabilities and mechanical properties in detail. Figure 1 depicted a cubic unit cell of $HgSm_2S/Se_4$ chalcogenides in a ball and polyhedral format having space group Fd-3m (227). Using the WIEN2k code, the studied spinel structure is built by positioning the Hg atom on lattice points (0.125, 0.125, 0.125), the Sm atoms on lattice points (0.5, 0, 0), and the S/Se atoms on lattice points (0.25, 0.25, 0.25). According to Murnaghan's state equation, it is exhibited (Fig. 2) that optimization pertains to the lowest ground state energy. By applying the formulae $\Delta E = E_{NM}-E_{FM}$, the energy difference is computed, which in turn validates the long-term viability of the examined compositions in the FM state. Consequently, one has come to know that the ferromagnetic state emits more energy than the nonmagnetic state. Likewise, ferromagnetic phases have been discovered to have greater stability per unit cell than non-magnetic phases and their calculated values are 21.14 eV and 25.62 eV for $HgSm_2Se_4$ and $HgSm_2S_4$ respectively.

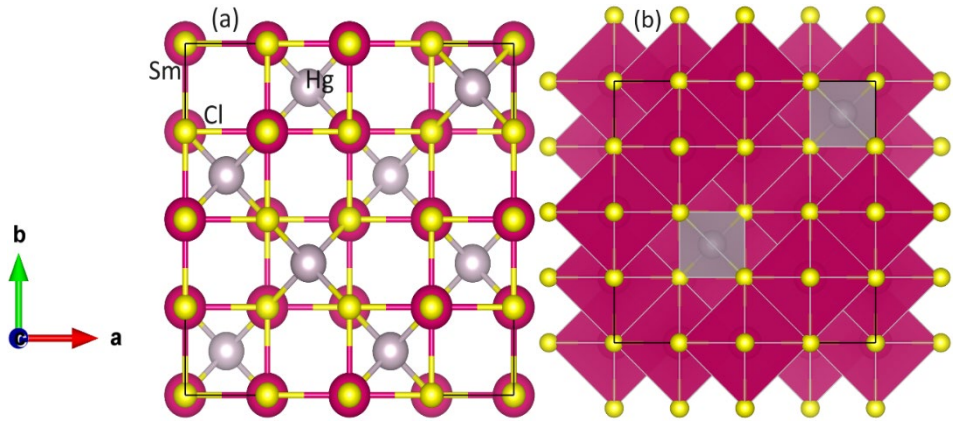

Fig. 1. Chalcogenides crystal structure of $HgSm_2S/Se_4$ (a) ball format and (b) polyhedral format Silver, red, and yellow ball show Hg, Sm, and S/Se atoms.

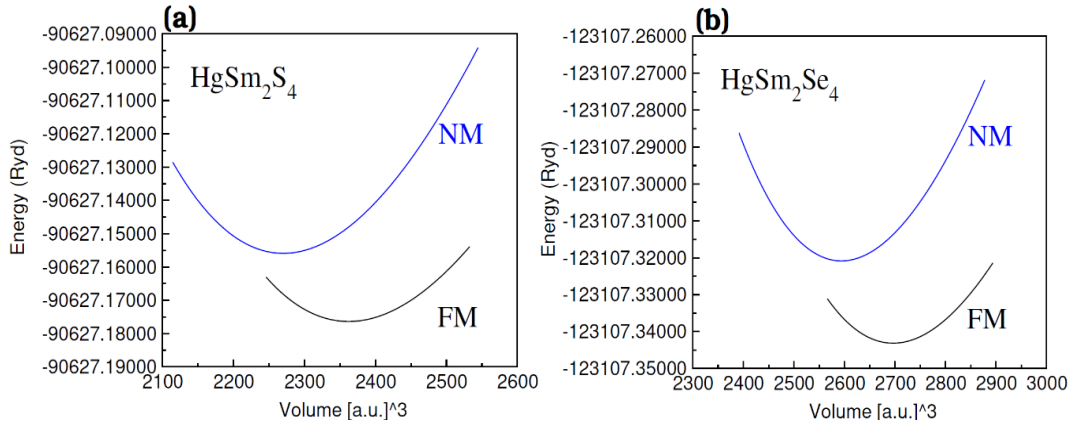

Fig. 2. (a) $HgSm_2S_4$ and (b) $HgSm_2Se_4$ compounds energy versus volume plot in ferromagnetic and non-magnetic phases.

In order to determine the reliability of concerned spinels in the FM phase, we additionally computed the ground-level energies of the ferromagnetic (FM) as well as anti-ferromagnetic (AFM) phases per unit cell. The retention of both spin orientations amongst the Sm elements has permitted for alignments throughout the AFM phase. To calculate the energy differences between the phases are estimated by applying the formula $\Delta E = E_{FM} - E_{AFM}$. Table 1 displayed the computed ΔE values, which indicated that AFM phases are not as durable as FM states. Heisenberg model and the mean-field technique $k_B T_C = \frac{2}{3}\Delta E$ played a vital role (by employing the connection) for estimating the T_c value [29, 30]. In the above equation, T_C, ΔE, k_B, are Curie temperature, energy differences, and Boltzmann constant, correspondingly. Table 1 revealed that the expected T_c values variated between 600-1000 K [31]. By summarizing the results, it's become clear that the larger the energy differences (ΔE), the greater will be Curie temperature Tc values.

Till now, there is not any experimental research history that would support a comparison of the aforementioned conclusions. The compounds' thermodynamic stability was ascertained by energy formation, or ΔH_f (refer to Table 1). The following is the equation for ΔH_f [32];

$$\Delta H_f = E_{\text{Total}}(\text{Hg}_l\text{Sm}_m S/Se_n) - \text{lE}_{\text{Hg}} - \text{mE}_{\text{Sm}} - \text{nE}_{S/Se} \quad (1)$$

$E_{\text{Total}}(\text{Hg}_l\text{Sm}_m S/Se_n)$ is the computed total ground state energy of the spinels under consideration. E_{Hg}, E_{Sm}, and $E_{S/Se}$ are the energies of individual atoms. The thermodynamic stability of the examined spinels is confirmed by the negative values of ΔH_f (see Table 1).

A decline is observed in ΔH_f values from -3.04 eV to -2.34 eV after swapping anions S with Se, which is a clear view of the exceptional thermodynamic stability of $HgSm_2S_4$. After the structures are optimized, a_0 and B_0 are calculated using Murnaghan's equation-of-state (depicted in Table 1). In both spinels, the a_0 grew while the B_0 declined. It results from the atoms' increasing separation with increasing anion sizes. The stability of studied compounds is confirmed by estimated values of formation energies.

Table 1. Optimized lattice constant (a_o(Å)), ground state bulk modulus (B_o(GPa)), Energy difference value (ΔE(eV), Curie temperature (T_c), Enthalpy energy ΔH_f(eV), Shear modulus G(GPa), Young Modulus Y (GPa):, B/G, υ and Anisotropy Factor for $HgSm_2Z_4$ (Z = S, Se).

Parameters	$HgSm_2S_4$	$HgSm_2Se_4$
	PBEsol-GGA	PBEsol-GGA
a_o(Å)	11.31	11.81
B_o(GPa)	62.88	51.90
ΔE(eV)	-66.40	-49.80
Tc	640	610
ΔH_f(eV)	-3.04	-2.34
C_{11}	84.05	67.48
C_{12}	52.65	44.18
C_{44}	14.05	10.95
B	63.11	51.94
G	14.68	11.22
Y	40.89	31.42
B/G	4.29	4.63
υ	0.39	0.40
A	0.89	0.93

For chalcogenide, spinels $HgSm_2S/Se_4$, the mechanical properties offer far more important information on structural stability [25, 33]. For instance, to evaluate the structural viability of the concerned compositions, the elastic constants are estimated via Tensor Matrix Analysis. It is claimed that for cubic structures, C_{11}, $C_{12,}$ and C_{44}, are the only requirements to assess systems. The Born criterion ($C_{11} + 2C_{12} > 0$, $C_{44} > 0$, $C_{12} < B_0 < C_{11}$, and $C_{11} - C_{12} > 0$) was implemented to ascertain that our compounds are stable [34]. The morphological durability in the concerned compositions was validated by acquired positive outcomes. The B_0 values acquired via graphs (optimized) using Murnaghan's equation-of-state and the relation $B_0 = (C_{11}+2C_{12})/3$ are comparable. The findings reported the durability of the spinel structure and supported the hypothesis that the elastic and structural characteristics are interrelated. A ductile character is necessary for materials to be employed in real-world uses. Poisson's ratio (υ) (with a critical limit of 0.26), measured how brittle and ductile the spinels are. The ductility of the compound is validated for $\upsilon < 0.26$. Brittleness is taken into consideration if the value is more than this limit value. The ductile character is confirmed by our computed Poisson's ratio values (>0.26) for $HgSm_2S_4$ and $HgSm_2Se_4$ (see Table 1). Moreover, The B_0/G (Pugh ratio) is also estimated for the confirmation of the studied compound's ductility trait with its critical limit of 1.75 [35, 36]. Besides this, the anisotropic (A) response is determined via Elastic Constant $A = 2C_{44}/(C_{11}–C_{12})$. If the magnitude of A is in proximity to unity, the spinels are considered as isotropic. If the compounds do not meet this criteria they may be regarded as anisotropic. Results conclude that both spinels are anisotropic as shown in Table 1.

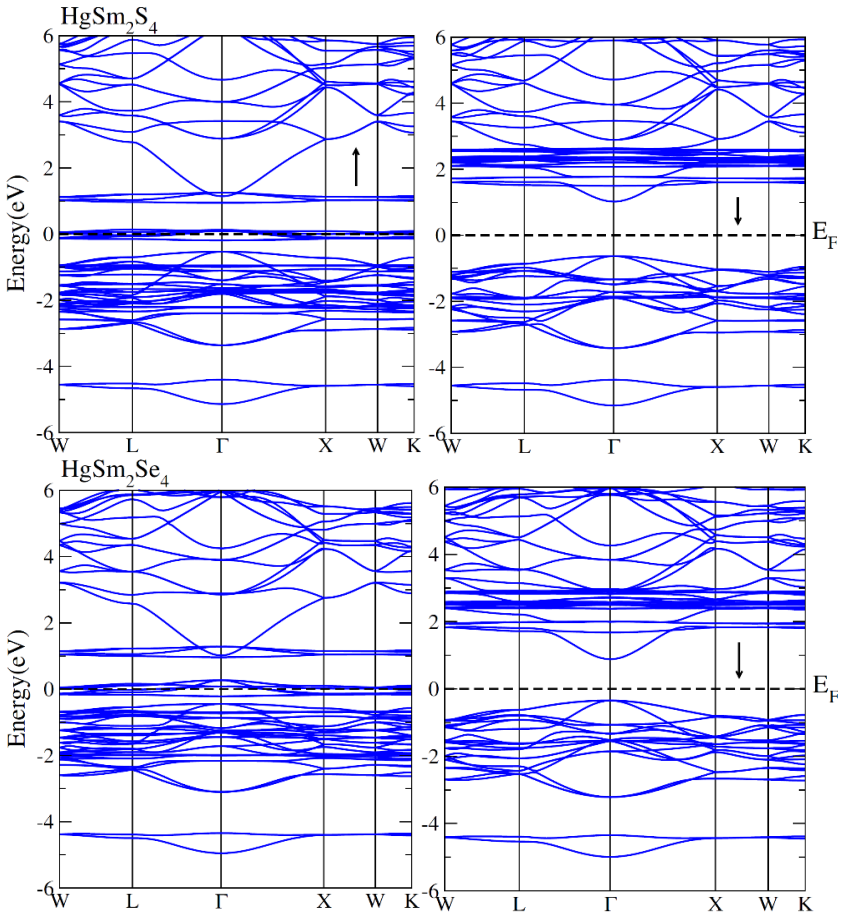

Fig. 3. Calculation of band structures for $HgSm_2S_4$ and $HgSm_2Se_4$ (in minority & majority spin channels).

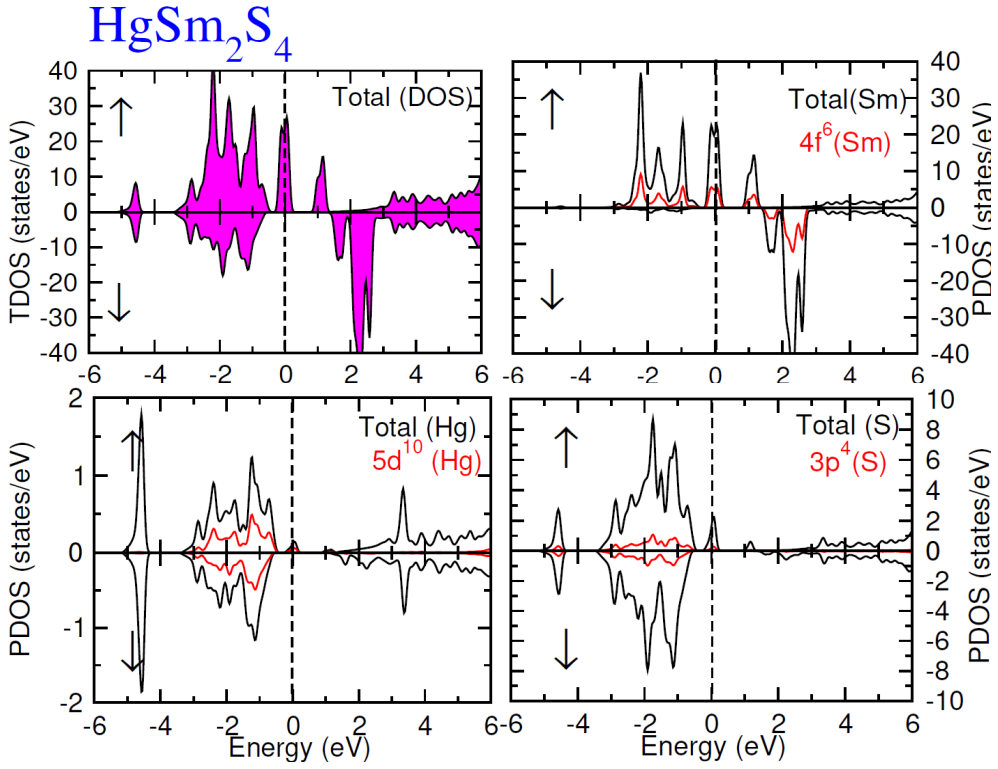

Fig. 4. TDOS and PDOS calculated for $HgSm_2S_4$ spinels (spin down (↓) and spin up (↑) orientation).

The optimized structures of $HgSm_2S/Se_4$ are used for the computation of band structures (BS) and DOS (density of states), and from these spin-oriented electronic characteristics are determined. The BS is assessed using modified Becke Johnson potentials (see Fig. 3). The Fermi-level in the BS figure appears at 0 eV. A metallic character has been incorporated into the spin-up channel and free charge carriers contribute as a result of the valence states overlapping the Fermi level. Contrarily, due to the collaboration of the Fermi level (in the spin-down medium) inside the forbidden gap, which resulted in the semiconductor trait. Consequently, the materials under investigation can be classified as half-metallic ferromagnetic, indicating that they ought to demonstrate full spin polarization. The computed spin-down gap ($\downarrow E_g$) values of $MgPr_2X_4$ compounds based on rare earth elements have shown comparable patterns to ferromagnetic semiconductors [37]. Figs. 4 and 5 displayed PDOS and TDOS trends in the limits of -3.1 eV to -1.0 eV and -3.4 eV to -4.0 eV for Hg, Sm, as well as S/Se, correspondingly. In contrast, its values for spin-down domains lie within -0.8 eV to -3.0 eV. In addition, hybridizing among Sm-4f, S/Se-p, and Hg-5d atomic orbitals took place in the conduction band (0.8 eV to 1.4 eV) during spin-up medium and between 1.6 eV and 2.8 eV in the spin-down module. For cubic spinels, theoretical approximations of the electronic properties known as valence and conduction band edges may be computed in various scenarios [38, 39].

In general, the verification of spinel stability is done by the fact that comparatively sufficient energy is liberated in the FM phase than in the AFM phase. Twofold exchange mechanism with an electrical exchange between down and up spin channels was additionally validated by the p-states and f-states hybridization amongst Sm and S/Se states. Furthermore, the replacement of energy across the channel resulting from FM bonding along with a decline in energy in FM states serve as supplementary means of verifying ferromagnetism. The magnetic moment was strongly generated by such magnetic compounds particularly composed of rare earth elements.

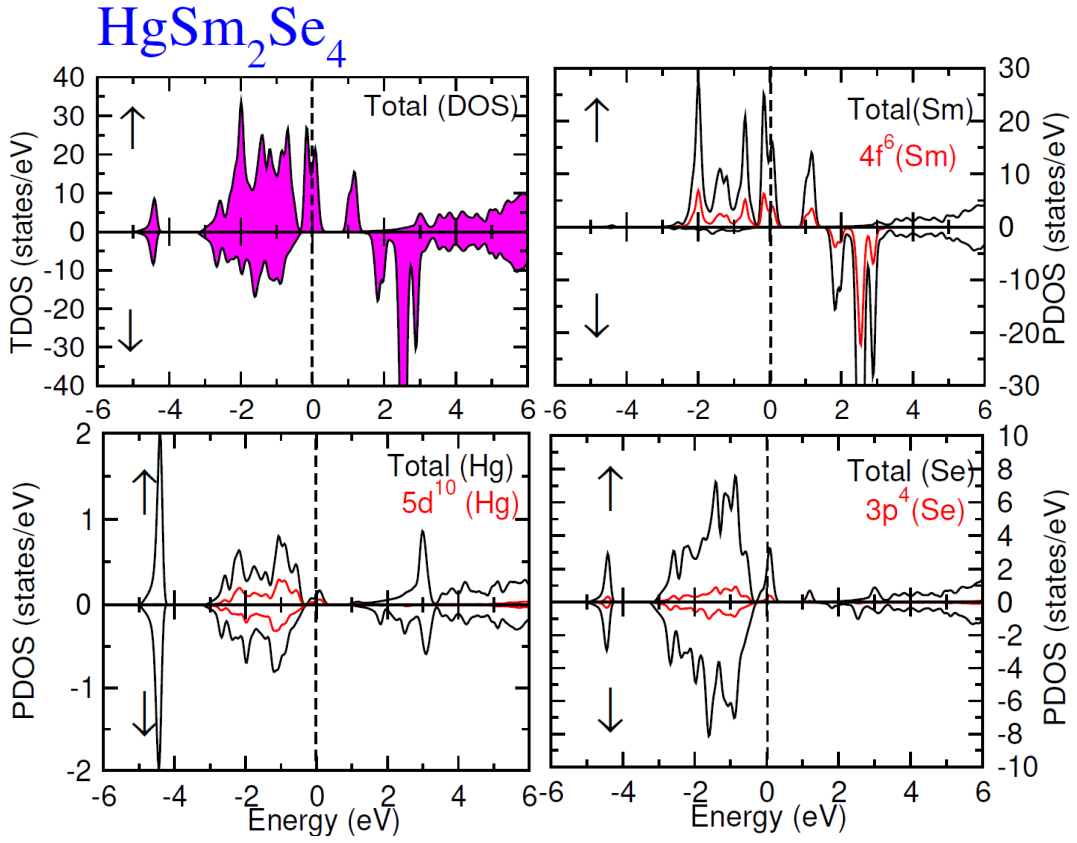

Fig. 5. TDOS and PDOS calculated for $HgSm_2Se_4$ spinels (spin down (↓) and spin up (↑) orientation).

Table 2 represented total magnetic moments (M_{tot}) and the local magnetic moments (M_{Sm}, M_{Se}, M_S, and M_{Hg}) that were determined using mBJ potential to ascertain the magnetic characteristics of $HgSm_2S/Se_4$. There was a clear link between the integer magnetic moment and electronic states moments in VB and CB. When combined with full spin polarization, this integer magnetic moment allowed for an easier comprehending view of spin orientation in up & down spin mediums. The magnetic field induced in Sm and other lanthanide-based materials is caused by lanthanides' f states. The inherent magnetic moments that exist in these elements are partly due to the existence of unbound e^-,s in f and d atomic orbitals. Remarkably, the computed value for $M_{tot}=10\mu_B$ corresponds to the fact that both spinels show ferromagnetic traits. The calculated values of local magnetic moments for the atoms of Se, S, and Hg, or μ_{Hg} μ_S, and μ_{Se}, are displayed in Table 2. The substantial coupling among Sm element's d orbitals and the p state of host semiconducting compounds produces moments on the S/Se and Hg positions. The calculations of M_{tot} and the individual magnetic moments of Sm atoms were comparable (refer to Table 2). Significant ferromagnetic exchange splitting produced the compounds' magnetic fields, and Sm acted as a magnetically receptive element. Moreover, a combination of S/Se and Hg components verified ferromagnetic properties in both compounds.

Table 2. Magnetic moments value for spinels $HgSm_2S_4$ and $HgSm_2Se_4$, total and their local M_{Hg}, M_{Sm}, and $M_{S/Se}$, interstitial ($M_{Int.}$).

	M_{Total}	$M_{Int.}$	M_{Hg}	M_{Sm}	$M_{S/Se}$
$HgSm_2S_4$	10.000	0.1125	0.006	5.054	-0.043
$HgSm_2Se_4$	10.000	0.0123	0.002	5.172	-0.085

4. Conclusion

The theoretical DFT-oriented current study extensively analyzed the mechanical, optical, thermoelectric, and magnetic characteristics of chalcogenide spinels $HgSm_2S/Se_4$. The diligent preference for the ferromagnetic state is highlighted by the cubic spinels' volume optimizations. Moreover, the determined energy formation is in favor of the spinels' strong foundation, which ideally preserves the magnetic phase. The thermodynamic and mechanical stabilities of both spinels have been verified by their respective parameters (negative enthalpy values and positive elastic constants). The calculated Pugh's and Poisson's ratios met the criteria of ductile nature which is more than 1.75 and 0.26, respectively. From BS calculations, the overall half-metallic nature absorbed due to the semiconducting nature in spin down and metallic nature in spin up is comparable to existing literature. A relatively solid ferromagnetic state is produced by the significant hybridization of component states as a consequence of exchange interactions. The marvelous results of the current study on chalcogenides highlighted novel applications employing spintronics technology.

Funding

Researchers Supporting Project number (RSPD2024R741), King Saud University

Acknowledgments

The authors would like to thank Researchers Supporting Project number (RSPD2024R741), King Saud University, Riyadh, Saudi Arabia.

References

[1] M. Liu, Z. Rong, R. Malik, P. Canepa, A. Jain, G. Ceder, K.A. Persson, Energy Environ. Sci. 8 (2015) 964-974; https://doi.org/10.1039/C4EE03389B

[2] Z. Rong, R. Malik, P. Canepa, G. Sai Gautam, M. Liu, A. Jain, K. Persson, G. Ceder, Chem. Mater. 27 (2015) 6016-6021; https://doi.org/10.1021/acs.chemmater.5b02342

[3] A. Wustrow, B. Key, P.J. Phillips, N. Sa, A.S. Lipton, R.F. Klie, J. T. Vaughey, K. R. Poeppelmeier, Inorg. Chem. 57 (2018) 8634-8638; https://doi.org/10.1021/acs.inorgchem.8b01417

[4] N.W. Grimes, The spinels: versatile materials. Phys. Technol. 6 (1975) 22; https://doi.org/10.1088/0305-4624/6/1/I02

[5] O. Vozniuk, T. Tabanelli, N. Tanchoux, J.M.M. Millet, S. Albonetti, F. Di Renzo, F. Cavani, Catalysts 8 (2018) 332; https://doi.org/10.3390/catal8080332

[6] G. Harbeke, H. Pinch, Phys. Rev. Lett. 17 (1966) 1090; https://doi.org/10.1103/PhysRevLett.17.1090

[7] N.A. Noor, M. Rashid, Ghulam M. Mustafa, Asif Mahmood, Waheed Al-Masry, Shahid M. Ramay, J. Alloys Compd., 856 (2021) 157198; https://doi.org/10.1016/j.jallcom.2020.157198

[8] H. Göbel, J. Magn. Magn. Mater. 3 (1976) 143- 146; https://doi.org/10.1016/0304-8853(76)90025-1

[9] A. Gaita-Ariño, F. Luis, S. Hill, E. Coronado, Nature chemistry, 11 (2019), 301-309; https://doi.org/10.1038/s41557-019-0232-y

[10] S. Sun, H. Zeng, D.B. S. Robinson, Raoux, P.M. Rice, S.X. Wang, G. Li, J. Am. Chem. Soc. 126 (2004) 273- 279; https://doi.org/10.1021/ja0380852

[11] Q. Mahmood, S. M. Alay-e-Abbas, M. Hassan, N.A. Noor, Journal of Alloys and Compounds, 688 (2016) 899-907; https://doi.org/10.1016/j.jallcom.2016.07.302

[12] T. Seddik, R. Khenata, A. Bouhemadou, N. Guechi. A. Sayede, D. Varshney, Y.Al-Douri, A.H. Reshak, S. Bin-Omran, Physica B 428 (2013) 78-88; https://doi.org/10.1016/j.physb.2013.07.014

[13] V. Samokhvalov, M. Dietrich, F. Schneider, S. Unterricker, Hyperfine Interactions 160 (2005) 17-26; https://doi.org/10.1007/s10751-005-9146-8

[14] Y.D. Park, A.T. Hanbicki, J.E. Mattson, B.T. Jonker, Appl. Phys. Lett. 81N8 (2002) 1471; https://doi.org/10.1063/1.1498503

[15] G. C. Lau, R. S. Freitas, B. G. Ueland, P. Schiffer, and R. J. Cava, Phys. Rev. B 72, (2005) 054411; https://doi.org/10.1103/PhysRevB.72.054411

[16] P. Lunkenheimer, R. Fichtl, J. Hemberger, V. Tsurkan, A. Loidl, Phys. Rev. B 72 (2005) 060103; https://doi.org/10.1103/PhysRevB.72.060103

[17] C.P. Sun, C.L. Huang, C.C. Lin, J.L. Her, C.J. Ho, J.Y. Lin, H. Berger, H.D. Yang, Appl. Phys. Lett. 96 (2010) 122109; https://doi.org/10.1063/1.3368123

[18] Y.M. Xie, Z.R. Yang, L. Li, L.H. Yin, X.B. Hu, Y.L. Huang, H.B. Jian, W.H. Song, Y.P. Sun, S.Q. Zhou, Y.H. Zhang, J. Appl. Phys.112 (2012) 12391; https://doi.org/10.1063/1.4770486

[19] R. von Helmolt, J. Wocker, B. Holzaphel, M. Scholtz, and K. Samwer, Phys. Rev Lett. 71 (1993) 2331; https://doi.org/10.1103/PhysRevLett.71.2331

[20] P. Bonnick, L. Blanc, S. H. Vajargah, C.-W. Lee, X. Sun, M. Balasubramanian, L. F. Nazar, Chem. Mater. 30 (2018) 4683-4693; https://doi.org/10.1021/acs.chemmater.8b01345

[21] J. Koettgen, C.J. Bartel, G. Ceder, Chemical Communications 56 (2020) 1952-1955; https://doi.org/10.1039/C9CC09510A

[22] P. Blaha, K. Schwarz, G.K.H. Madsen, D. Kvasnicka, J. Luitz, WIEN2K, An Augmented Plane Wave + local Orbitals Program for Calculating Crystal Properties, Karlheinz Schwarz, Techn. Universiïat Wien, Austria, 2001

[23] Maiza Zanib, N.A. Noor, M.A. Iqbal, I. Mahmood, Asif Mahmood, Shahid M Ramay, Najib YA Al-Garadi, Tariq Uzzaman, Current Appl. Phys. 20 (2020) 1097-1102; https://doi.org/10.1016/j.cap.2020.07.003

[24] Asif Mahmood, M. Rashid, KanzaSafder, M. Waqas Iqbal, N.A. Noor, Shahid M. Ramay, Waheed Al-Masry, NajibY.A.Al-Garadi, Res. Phys. 20 (2021) 103709 https://doi.org/10.1016/j.rinp.2020.103709

[25] P. Perdew, A. Ruzsinszky, G. I. Csonka, O. A. Vydrov, G. E.Scuseria, L. A. Constantin, X. Zhou, K. Burke, Phys. Rev. Lett. 100 (2008) 136406; https://doi.org/10.1103/PhysRevLett.100.136406

[26] F. Tran, P. Blaha, Phys. Rev. Lett. 102 (2009) 226401; https://doi.org/10.1103/PhysRevLett.102.226401

[27] Kin Mun Wong, S. M. Alay-e-Abbas, Yaoguo Fang, A. Shaukat, Yong Lei, Journal of Applied Physics 114 (2013) 034901; https://doi.org/10.1063/1.4813517

[28] S.M. Alay-e-Abbas, F. Javed, Ghulam Abbas, Nasir Amin, AmelLaref, J. Phys. Chem. C 123 (2019) 6044-6053; https://doi.org/10.1021/acs.jpcc.8b12221

[29] J Kudrnovský, I Turek, V Drchal, F Máca, P Weinberger, Phys. Rev. B 69 (2004) 115208; https://doi.org/10.1103/PhysRevB.69.115208

[30] F Máca, J Kudrnovský, V Drchal,G. Bouzerar, Appl. Phys. Lett. 92 (2008) 212503; https://doi.org/10.1063/1.2936858

[31] W.Z. Xiao, G. Xiao, Q.Y. Rong, Q. Chen, L.L. Wang, J. Magn. Magn. Mater. 438 (2017) 152-62; https://doi.org/10.1016/j.jmmm.2017.04.090

[32] B.R. Nag, Electron Transport in Compound Semiconductors; Springer Science & Business Media, 2012; Vol. 11.

[33] W Tahir, GM Mustafa, NA Noor, SM Alay-e-Abbas, Q. Mahmood, A. Laref, Ceramics International, 46 (2020) 26637-26645; https://doi.org/10.1016/j.ceramint.2020.07.133

[34] Farzana Majid, M. Tauqeer Nasir, Eman Algrafy, Muhammad Sajjad, N.A. Noor, Asif Mahmood, Shahid M.Ramay, J. Mat. Res. Tech. 9 (2020) 6135-6142; https://doi.org/10.1016/j.jmrt.2020.04.016

[35] X. Ji, Y. Yu, J. Ji, J. Long, J. Chen, D. Liu, J. Alloy Compd. 623 (2015)304; https://doi.org/10.1016/j.jallcom.2014.10.151

[36] Q. Mahmood, G. Murtaza, R. Ahmad, T. Hussain, I.G. Will, Curr. Appl. Phys. 16 (2016) 361-370; https://doi.org/10.1016/j.cap.2015.12.024

[37] A. Mahmood, M. Rashid, K. Safder, M.W. Iqbal, N.A. Noor, Shahid M. Ramay, Waheed Al-Masry, and Najib YA Al-Garadi. Results in Physics 20 (2021) 103709; https://doi.org/10.1016/j.rinp.2020.103709

[38] M. Roknuzzaman, K. Ostrikov, H. Wang, A. Du, T. Tesfamichael, Sci. Reports 7(2017) 14025; https://doi.org/10.1038/s41598-017-13172-y

[39] G. Hayatullah, R. Murtaza, S. Khenata, S. Mohammad, M.N. Naeem, A. Khalid, Manzar, Phys. B 420 (2013) 15; https://doi.org/10.1016/j.physb.2013.03.011